ACS APPLIED MATERIALS & INTERFACES

Research Article

www.acsami.org

Simultaneous Enhancements of UV Resistance and Mechanical Properties of Polypropylene by Incorporation of Dopamine-Modified Clay

Si Lei Phua,[†] Liping Yang,[†] Cher Ling Toh,[†] Ding Guoqiang,[†] Soo Khim Lau,[‡] Aravind Dasari,[†] and Xuehong Lu*,[†]

[†]School of Materials Science and Engineering, Nanyang Technological University, 50 Nanyang Avenue, Singapore 639798

[‡]Singapore Institute of Manufacturing Technology, 71 Nanyang Drive, Singapore 638075

Supporting Information

ABSTRACT: Inspired by the radical scavenging function of melanin-like materials and versatile adhesive ability of mussel-adhesion proteins, dopamine-modified clay (D-clay) was successfully incorporated into polypropylene (PP) using an amine-terminated PP oligomer as the compatibilizer. Although the PP/D-clay nanocomposites exhibit intercalated morphology, the incorporation of D-clay greatly improves the thermo-oxidative stability and UV resistance of PP owing to the strong radical scavenging ability of polydopamine (PDA) and large contact area between PP and the PDA coating on clay mineral. Moreover, the reinforcement effect brought by D-clay is fairly significant at very low clay loadings probably owing to the strong interfacial interactions between the layered silicates and the compatibilizer as well as that between the compatibilizer and the PP matrix. The work demonstrates that D-clay is a type of promising nanofiller for thermoplastics used for outdoor applications since it stabilizes and reinforces the polymers simultaneously.

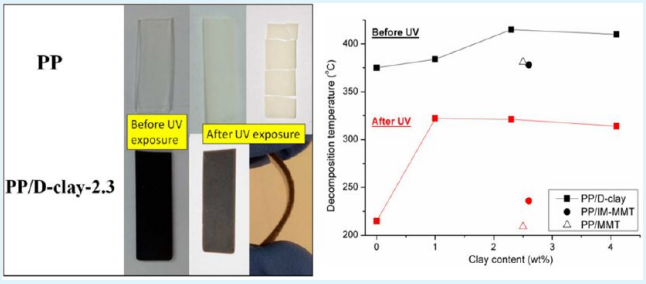

KEYWORDS: *polydopamine, polypropylene, clay, UV resistance, mechanical properties*

INTRODUCTION

Polymer/clay nanocomposites have received great attention in the past three decades owing to their light weight coupled with significantly better mechanical and barrier properties than the corresponding neat polymer resins.[1−4] Still, the practical use of these materials also depends on their service life in application environments, especially in outdoor environments where ultraviolet (UV) irradiation may induce severe photodegradation of polymers. Traditionally, organic surfactants with long alkyl chains are used to modify clay surfaces to improve the compatibility of polymer matrixes with clay mineral and facilitate its exfoliation. On the other hand, these organic small molecules are susceptible to breaking down into free radicals in high-temperature[5] or outdoor environments through thermo-oxidative and photo-oxidative reactions, accelerating the degradation of the polymer matrixes.[6,7] Furthermore, such organic surfactants provide relatively weak interactions, van der Waals interactions in most cases, between polymer matrixes and organoclay, leading to relatively poor interfacial stress transfer.[8]

Polydopamine (PDA) is a biomimetic synthetic polymer that has attracted strong interest recently as a universal surface modification agent for use in a wide range of applications owing to its superior adhesion properties and ease of preparation.[9−11] It has been reported that PDA can act as free-radical scavenger as its chemical structure is similar to that of eumelanins,[12−14] which are well known natural pigments for the protection of human body against UV by quenching reactive radicals generated by exposure to UV.[12] It has also been reported that the thermal degradation of poly(methyl methacrylate) and polypropylene (PP) by radical-initiated chain scission could be drastically lessened by incorporating 0.5−5 wt % melanin-like nanoparticles.[13] In the presence of reactive oxygen species and radicals, melanin can be easily oxidized to the corresponding quinone, quenching the reactive species by hydrogen atom transfer, and this radical scavenging reactivity can be further enhanced by the presence of metal ions, such as Mg^{2+}.[15] Other than the radical scavenging capability, recent studies also revealed that the photoprotective function of melanin-like macromolecules is related to its ability to absorb harmful radiation and dissipate the energy very efficiently via non-radiative paths.[12,16,17] It is believed that PDA is able to protect the surrounding substances under hostile sunlight exposure by acting as radical scavenger and sunscreen. Besides, the reactivities of PDA with different types of clay minerals have been reported.[18−20] Messersmith et al. demonstrated that the

Received: October 23, 2012
Accepted: January 28, 2013
Published: January 29, 2013

catechol groups in PDA can adhere to inorganic surfaces such as metal oxide and silica surfaces by forming coordination chelate bonds and the binding force of three to four such bonds can surpass a covalent bond.[21] PDA is also capable of interacting strongly with polymers via hydrogen bonds[11] and covalent bonds[10] and, hence, can serve as an effective stress transfer agent at organic−inorganic interfaces.[22] Our previous work has demonstrated that PDA could be facilely coated on nanofillers such as montmorillonite and graphene, and this indeed enhanced interfacial interactions between the nanofillers and polymer matrixes.[8,23−25]

On the basis of the above work, we hypothesized that if dopamine-modified clay (D-clay) is incorporated into polymers that degrade via radical-initiated chain scission, the D-clay nano-platelets may act as free-radical scavenger and harmless photon absorber to work against thermo-oxidative and UV-induced degradation, in addition to act as reinforcing nanofillers. The radical scavenging efficiency of PDA may also be improved as D-clay with nearly a monolayer of PDA on the surface will provide larger contact areas between PDA and the polymers than PDA nanoparticles. In this work, polypropylene (PP)/D-clay was chosen as the model system to verify the hypothesis because PP is commonly used in outdoor environments, and it is prone to processing-induced and UV-induced radical degradation[26] due to the presence of unstable tertiary hydrogens.[13] In order to improve the compatibility between apolar PP and D-clay, an amine-terminated PP oligomer ($PPNH_2$) is used as the compatibilizer since the amine groups could help the PP oligomer molecules be anchored onto the PDA coating through Michael addition and strong hydrogen bonding.[10] Herein, we demonstrate the significant simultaneous stabilizing and reinforcing effects of D-clay in the PP nanocomposites.

EXPERIMENTAL SECTION

Materials. Pristine PGW-grade sodium montmorillonite (MMT) with cationic exchange capacity of 145 mmol/100 g was obtained from Nanocor, Inc (Arlington Heights, USA). Tris(hydroxymethyl)-aminomethane (TRIS, 99%), dopamine hydrochloride (DOPA-HCl, 98%), and 2,2-diphenyl-1-picrylhydrazyl (DPPH) were purchased from Sigma-Aldrich and used as received. Maleic anhydride-terminated PP (PPMA, M_n = 8000, melting point = 140 °C, acid number = 15) was kindly provided by Baker Hughes (Houston, TX). Ethylenediamine (EDA, purum grade) was purchased from Fluka. PP (Cosmoplene H101E, melt flow index = 3.5 g/10 min, density = 0.9 g/cm^3) was purchased from Polyolefin Company (Singapore) Pte. Ltd. 1-Hexadecyl-2,3-dimethylimidazolium chloride (IM) was obtained from Merck, Germany. Toluene and dimethylformamide (DMF, ACS grade) were obtained from Tedia while acetone and methanol (technical grade) were obtained from Aik Moh and used without further purification.

Preparation of D-Clay, $PPNH_2$, and the Nanocomposites. D-Clay was prepared using the method reported in our previous publication[8] and re-dispersed in toluene by ultrasonication. The synthesis of PP/D-clay consisted of three steps: (I) synthesis of $PPNH_2$, (II) solution mixing of $PPNH_2$ and D-clay, and (III) melt compounding of $PPNH_2$/D-clay with PP. In step I, 30 g of PPMA was dissolved in 350 mL of toluene at 120 °C and refluxed overnight, followed by adding 1.35 g of ethylenediamine (PPMA/EDA molar ratio = 1/6) into the solution and continuing the reaction for another 24 h. The resultant $PPNH_2$ was then precipitated in methanol and dried under vacuum at 70 °C for 1 day. In step II, $PPNH_2$ was intercalated into clay interlayers via solution mixing. Both D-clay and $PPNH_2$ were dispersed in toluene and mixed at $PPNH_2$/MMT weight ratio of 3/1 at 120 °C in N_2 environment for 3 days. The product was then precipitated in methanol and dried under vacuum at 70 °C for 1 day. Finally, calculated amounts of $PPNH_2$/D-clay powders were mixed with PP pellets by melt compounding using a PRISM twin screw extruder at 190 °C. Trialkylimidazolium-modified clay (IM-MMT) was prepared using the method reported in our previous publication.[27] Both IM-MMT and pristine MMT were dried at 80 °C overnight prior to compounding with PPMA and then with PP to make reference materials PP/IM-MMT and PP/MMT. In both cases, the weight ratio of PPMA/MMT was fixed at 3/1. Pure PP was also extruded under the same condition as a reference. PDA particle was prepared as a reference by self-polymerization of DOPA without MMT for 24 h in Tris buffer, the suspension was centrifuged and washed by acetone for 4 times, followed by drying in a vacuum oven at 50 °C for 48 h.

Characterization. The clay contents in the nanocomposites were determined by thermo-gravimetric analysis (TGA) using TA Instrument TGA Q500. The specimens were heated from 25 to 850 °C at 10 °C/min in air (sample purge rate = 60 mL/min). On the basis of the TGA results, the nanocomposite samples are designated as PP/D-clay-1.0, PP/D-clay-2.3, PP/D-clay-4.1, PP/IM-MMT-2.6, and PP/MMT-2.5, respectively, where the numbers indicate the weight percentages of MMT. Decomposition temperature (T_d) is defined as the temperature at 5 wt % weight loss. The structures and morphologies of the nanocomposites were characterized using wide angle X-ray diffraction (WAXD) and transmission electron microscopy (TEM). The films were scanned at room temperature from 2θ = 2° to 30° at a scanning rate of 1°/min using a PANalytical X'Pert PRO diffractometer with Cu Kα radiation. TEM was performed using a JOEL 2100 TEM at 200 kV. The samples (thin films with 1 mm thickness) were microtomed using Leica Ultracut UCT into about 50−100 nm thickness at −60 °C. The onset oxidation temperature (OOT) was determined according to ASTM E2009 using TA Instrument DSC 2010. To study the photostability of the samples, thin films of 0.3−0.33 mm thickness were irradiated with UV light for 3 weeks using RPR-200 (Rayonet) with light intensity of 92 W/m^2 at the center of the reactor. The surface topography of degraded samples was observed with an Olympus BX53 optical microscope at a magnification of 4×. Thermal degradation temperatures of the samples were measured by heating the samples from 25 to 850 °C in nitrogen (sample purge rate = 60 mL/min). FTIR measurements were performed using a Shimadzu FTIR IR Prestige-21 equipped with Golden Gate ATR accessory. Each sample was scanned 32 times at a resolution of 4 cm^{-1}. All the spectra for photodegradation study are normalized at 2722 cm^{-1} which is associated with CH_3 stretching and CH bending.[28] The thermal behaviors of the unexposed and UV-exposed nanocomposites were characterized using differential scanning calorimetric (DSC) performed on a TA Instrument DSC Q10 at a heating rate of 10 °C/min, and the second melting was taken for analysis. The radical scavenging activity of D-clay was evaluated by DPPH assay according to the method reported in the literature[14] with slight modifications. DPPH solution (0.01 mM) in DMF was freshly prepared prior to usage, followed by adding 150 μL of D-clay suspension (1 mg/mL in DMF) into 3 mL of DPPH solution. The scavenging activity was measured by monitoring the absorbance change at 516 nm at different times in the dark with a UV-2501PC spectrophotometer (Shimadzu). DPPH radical scavenging activity was calculated as $I = [1 - (A_i - A_s)/A_{dpph}] \times 100\%$, where A_{dpph} is the absorbance of the DPPH without D-clay, A_i is the absorbance of the DPPH with D-clay measured at different time, and A_s is the absorbance of D-clay itself without the DPPH solution. In order to compare the scavenging efficiency of D-clay with that of PDA, based on the fact that the PDA content in D-clay is about 20 wt %,[8] 0.2 mg/mL of PDA in DMF and 0.8 mg/mL of clay in DI water were also prepared and 150 μL of each suspension was used for testing. The tensile properties were measured using an Instron 5567 machine according to ASTM D638 type V at a crosshead speed of 25 mm/min using injection-molded dog-bone specimens (ASTM Type V in 1 mm thickness, 500 N load cell). The crystallinity of the molded tensile samples was studied using modulated DSC (MDSC) on a TA Instrument DSC 2920 at a heating rate of 5 °C/min with a temperature amplitude of 0.796 °C over a period of 60 s. The percent crystallinity (X_c) was calculated by subtracting the reversing heat flow

Scheme 1. Schematic Illustration of the Preparation Route of PP/D-Clay Nanocomposites

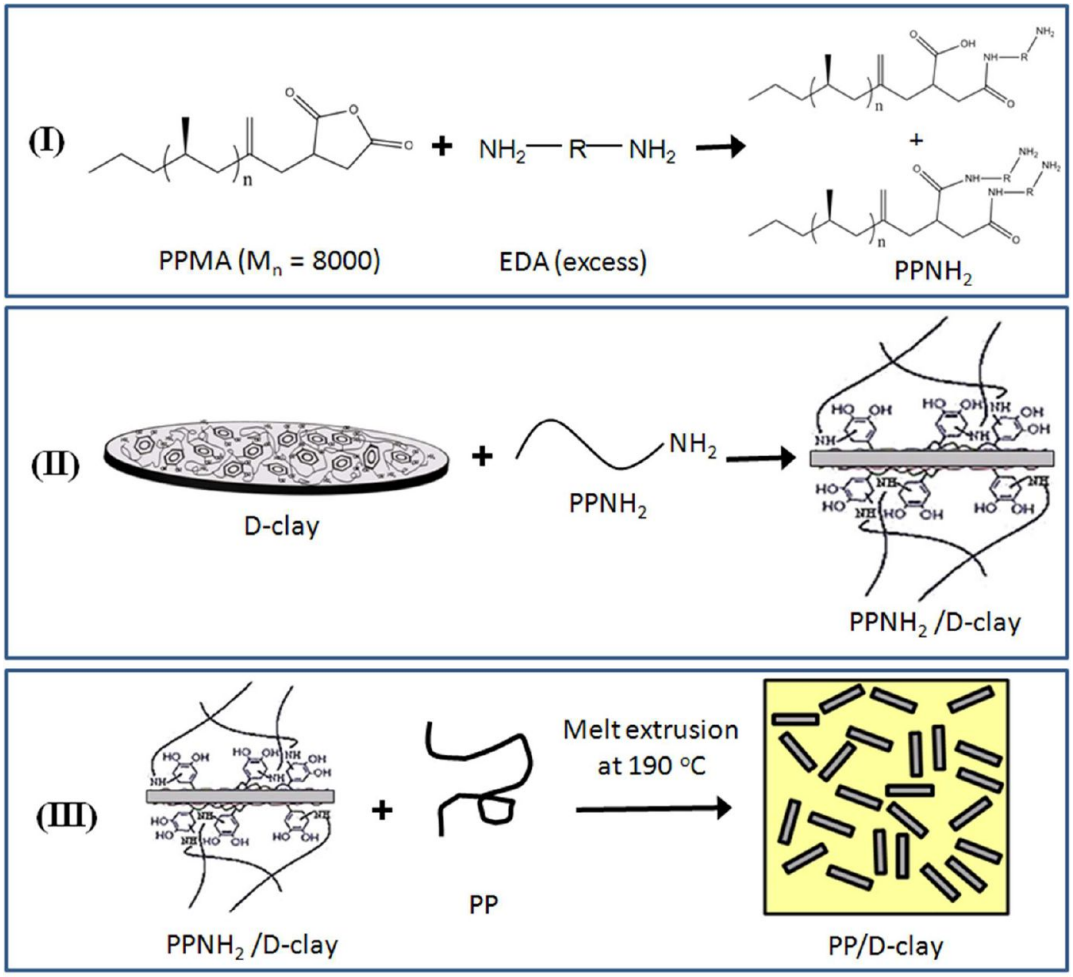

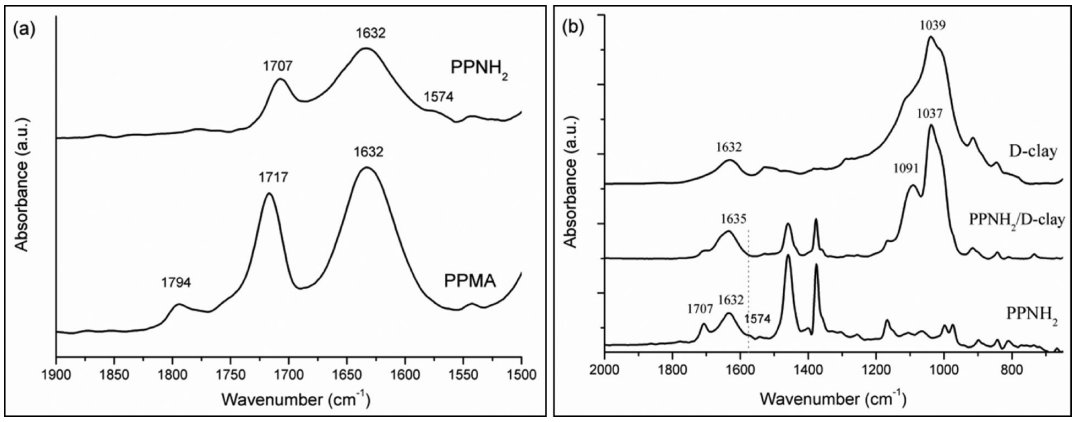

Figure 1. FTIR spectra of (a) PPMA and $PPNH_2$ and (b) $PPNH_2$, D-clay, and $PPNH_2$/D-clay.

from the nonreversing heat flow and dividing by the heat of fusion for 100% crystalline PP (209 J/g).[26]

RESULTS AND DISCUSSION

Preparation and Morphology of the PP/D-Clay Nanocomposites. In this work, terminal-functionalized PP oligomers were used as the compatibilizer as the terminal functional groups can facilely interact with clay platelets without much steric hindrance[29] while the relatively long PP tails (M_n = 8000) may entangle with the PP matrix, facilitating clay dispersion. In order to obtain a stronger interface, we converted maleic anhydride-terminated PP (PPMA) to amine-terminated PP ($PPNH_2$) since a primary amine group has two hydrogen donors and hence may form stronger hydrogen bonds and probably also chemical bonds through Michael addition[10] with the PDA coating on clay (Scheme 1).

For the step I, the successful synthesis of $PPNH_2$ is verified by the FTIR spectra shown in Figure 1a. The maleic anhydride (MA) group in PPMA is transformed into amide linkage after the reaction with the diamine.[30] This is evidenced by the

dx.doi.org/10.1021/am3024405 | ACS Appl. Mater. Interfaces 2013, 5, 1302−1309

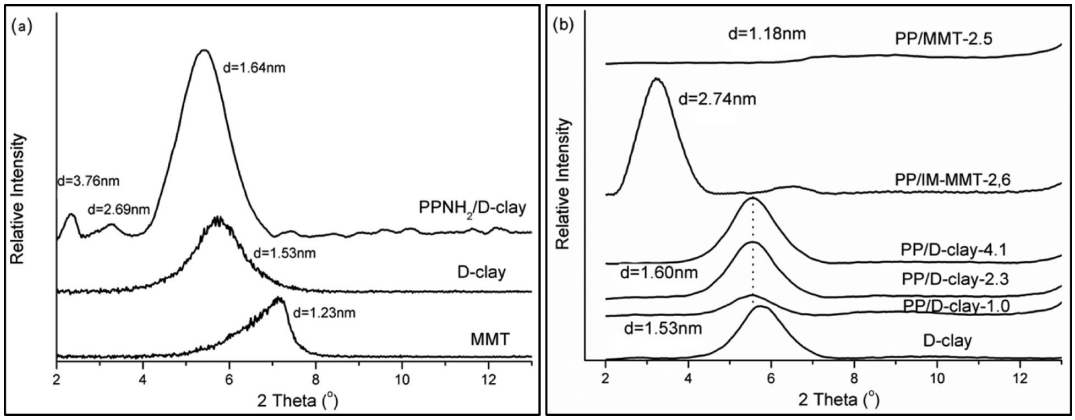

Figure 2. WAXD patterns of (a) pristine clay, D-clay, and $PPNH_2$/D-clay and (b) the nanocomposites. The numbers in the sample names indicate the weight percentages of MMT.

disappearance of the bands corresponding to the MA group at 1794 and 1717 cm^{-1} in the $PPNH_2$ spectrum and the formation of the new band at 1707 cm^{-1} and a hump at 1574 cm^{-1} that can be attributed to the carbonyl group of amide linkage and N−H bending, respectively.[31] For the step II, the split of Si−O band into two bands at 1091 and 1037 cm^{-1} for $PPNH_2$/D-clay (Figure 1b) indicates the enlarged separation between clay layers owing to the intercalation by $PPNH_2$.[32] The absence of the N−H bending band at 1574 cm^{-1} in the spectrum of $PPNH_2$/D-clay suggests that a considerable amount of amine groups of $PPNH_2$ may have reacted with the PDA coating. The WAXD patterns of D-clay and $PPNH_2$/D-clay (Figure 2a) confirm that $PPNH_2$ chains can diffuse into the D-clay interlayer spaces due to the favorable interactions between the PDA coating and $PPNH_2$, resulting in a slight expansion of the interlayer *d*-spacing from 1.53 nm (2θ = 5.77°) for D-clay to 1.64 nm (2θ = 5.38°) for $PPNH_2$/D-clay. The TEM images of $PPNH_2$/D-clay confirm the presence of intercalated clay stacks that are well dispersed in the matrix, as shown in Figure S1, Supporting Information. Upon the compounding (step III), PP/D-clay shows almost the same interlayer spacing with that of D-clay/$PPNH_2$, implying that the compounding process does not further promote D-clay intercalation. To compare with PP/D-clay nannocomposites, two reference samples, i.e., PP/pristine clay (PP/MMT) and PP/trialkylimidazolium-modified clay (PP/IM-MMT), were also prepared. PP/MMT shows almost the same interlayer spacing with that of the pristine clay, as expected, due to the poor compatibility between PP and the pristine clay. On the contrary, the *d*-spacing of IM-MMT is expended from 2.2 nm for the as-prepared IM-MMT[27] to 2.74 nm (2θ = 3.22°) after the compounding, signifying a better intercalation of IM-MMT by PP than D-clay. Consistent with the WAXD data, TEM images in Figure 3 also show that, at similar clay content, IM-MMT is dispersed slightly better in PP than D-clay since some very thin clay stacks or even single layers could be observed in the PP/IM-MMT nanocomposite whereas they are almost absent in the corresponding PP/D-clay nanocomposite. This is probably because the relatively weak interactions between IM-MMT layers make them easier to be exfoliated by shearing during the compounding process. In contrast, the strong interactions between D-clay layers make D-clay stacks more difficult to be further exfoliated.[25]

Thermo-Oxidative Stability and UV Resistance of PP/D-Clay Nanocomposites. It is widely accepted that the

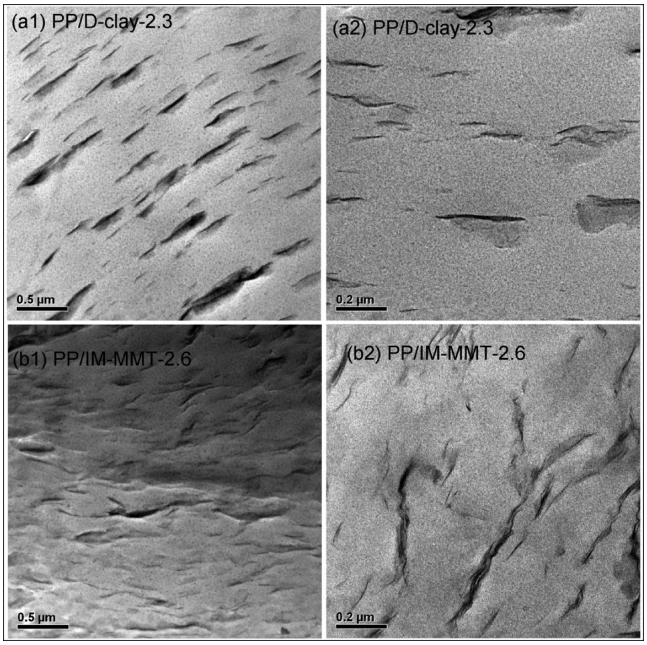

Figure 3. Typical TEM images of (a1, a2) PP/D-clay-2.3 and (b1, b2) PP/IM-MMT-2.6 nanocomposites.

incorporation of clay minerals into polymers would improve the thermal-oxidative stability of the nanocomposites owing to Labyrinth barrier effect, which is highly dependent on clay dispersion. From Figure 4a, we can see that PP/MMT has lower T_d than that of neat PP due to the catalytic effect of the unmodified layered silicates[6] and the poor clay dispersion. In contrast, the T_d of both PP/IM-MMT and PP/D-clay nanocomposites increases with clay content. This can be attributed to the formation of a silicate barrier layer during decomposition, which hinders the diffusion of oxygen into and also the diffusion of the volatile decomposition products out of the nanocomposites.[7] For the nanocomposites with good clay dispersion, thicker barrier layer may be formed with increasing clay content, delaying the thermal decomposition. However, although the dispersion of IM-MMT in PP is better than that of D-clay, the increase in T_d brought by D-clay is more pronounced. Since PP contains unstable tertiary hydrogens and hence degrades rapidly at elevated temperature upon radical attack,[13] the above results suggest that the PDA coating on clay can scavenge the chain end radicals by hydrogen atom

dx.doi.org/10.1021/am3024405 | ACS Appl. Mater. Interfaces 2013, 5, 1302−1309

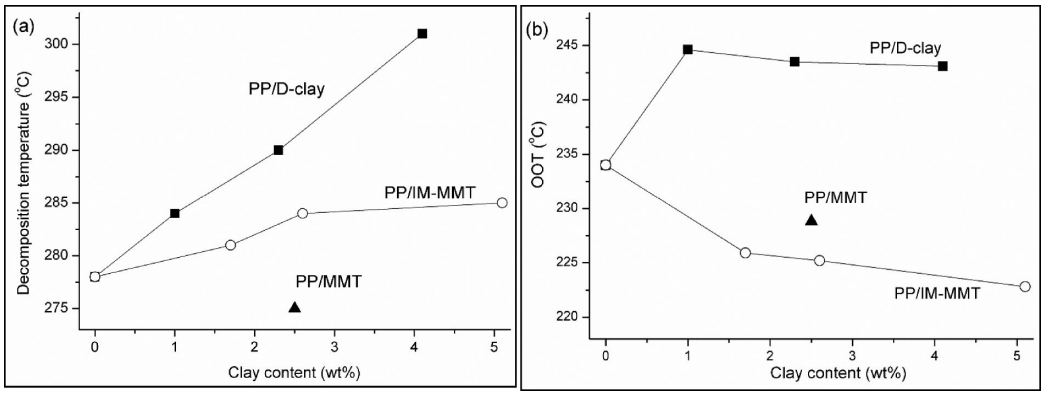

Figure 4. (a) Thermal decomposition temperatures (T_d) in air and (b) oxidative onset temperature (OOT) of PP, PP/D-clay, PP/IM-MMT, and PP/MMT nanocomposites. T_d is defined as the temperature at 5 wt % of weight loss.

transfer[15] and hence block the chain scission. Although trialkylimidazolium-modified clays are more thermally stable than quaternary alkylammonium-modifed clay,[33] IM-MMT could not interfere with the chain scission reactions of PP. The combined effects of the radical scavenging and the char formation by silicate layers give rise to a more impressive increase in T_d at higher D-clay contents.

The stabilizing effect of D-clay is further verified by the onset oxidation temperatures (OOT) of the samples (cf. Figure S2, Supporting Information). Unlike T_d that depends on the evaporation of the decomposed products and hence the barrier effect of layered silicates, OOT reflects the thermo-oxidative stability of the materials more directly and is a more useful parameter for processing and applications.[7] Figure 4b shows that OOT of the PP/D-clay nanocomposites is 10 °C higher than that of neat PP. On the contrary, OOT of PP/IM-MMT is lower than that of neat PP. This clearly demonstrates that, while organoclay promotes the thermo-oxidative degradation, D-clay can delay the thermo-oxidative degradation owing to the free-radical scavenger ability of the PDA coating. Unlike the trend observed for T_d, for both PP/D-clay and PP/IM-MMT, OOT does not increase with increasing clay content. This is probably due to the increased amount of $PPNH_2$ and PPMA with increasing clay content, which deteriorates the stabilizing effect of clay on PP.

Since PP is also prone to sunlight-induced radical degradation, there is also a growing interest to improve its UV resistance.[26,28] Although a good dispersion state of layered silicates may also be a benefit to photostability because of the barrier effect,[34] it has been reported that both organoclay and PPMA compatibilizer accelerates the photodegradation of PP due to the presence of active species in clay minerals and the unstable anhydride units, respectively.[6,35] To prove that D-clay can also enhance the photostability of PP, all samples were exposed to UV irradiation intensively. After the UV exposure for 3 weeks, an intense, broad infrared absorption band is detectable in the range of 1700−1800 cm^{-1} for UV-exposed PP, PP/IM-MMT, and PP/MMT (Figure 5a(i)), which can be assigned to carbonyl species as a result of severe degradation. As reported in the literature, at the beginning of the photodegradation, the absorption band of carboxylic acid was initially observed at 1712 cm^{-1}, followed by the appearance of the bands corresponding to ketones and lactones (at 1720 and 1780 cm^{-1}) with exposure periods longer than 60 h.[6,26] The broad band in the range of 1700−1800 cm^{-1} can be attributed to overlapping of the different carbonyl bands. It is striking to observe that the carbonyl absorption bands for the UV-exposed PP/D-clay nanocomposites are very weak (Figure 5a(ii)), indicating that D-clay can effectively act as free radical scavenger and harmless photon absorber to stabilize the PP chains and lessen the photoinduced degradation. It is worth noting that the UV-exposed PP/D-clay-1.0, which contains only about 0.2 wt % PDA, shows almost no carbonyl absorption band, indicating the high efficiency of D-clay as photoprotectant.

The extent of photodegradation is further investigated by measuring the T_ds of the samples before and after the UV exposure. After the UV exposure, the T_ds of neat PP, PP/MMT, and PP/IM-MMT all decrease drastically (Figure 5b) due to the radical-initialized chain scission. Impressively, the T_ds of PP/D-clay-1.0 and PP/D-clay-2.3 are 100 °C higher than that of neat PP and PP/MMT and 85 °C higher than that of PP/IM-MMT after the UV treatment. Consistent with the TGA results, melting points (T_m) of UV-exposed PP/D-clay are much higher than the other counterparts owing to lower extent of photodegradation (Figure 5c). Figure 5d demonstrates that PP/D-clay-2.3 still retains some flexibility after the hostile UV treatment for 2 months. In contrast, the neat PP sample becomes too brittle to be handled due to the large surface cracks formed, as shown in Figure 6. Normally, surface cracks are formed due to the contraction of the surface layer as a result of photodegradation, leading to severe depreciation in mechanical properties of photodegraded products.[26] Obviously, the cracks on the surface of UV-PP/D-clay-2.3 are much finer than that on neat PP, PP/MMT-2.5, and PP/IM-MMT-2.6 surfaces, and hence, PP/D-clay nanocomposites are still fairly tough even after hostile UV treatment. All the results shown above consistently indicate that the photostability of PP/D-clay is much more superior to unfilled PP and the other PP/clay nanocomposites.

The radical scavenging activity of D-clay was further evaluated with the DPPH assay. Figure 7a shows that the absorbance at 516 nm, which corresponds to absorption band of DPPH radicals, decreases with increasing time upon the addition of D-clay to the DPPH solution. Evidently, the radical scavenging efficiency of D-clay is significantly higher than PDA particles (Figure 7b), which may be attributed to the larger surface area of the PDA coating on clay. The radical scavenging mechanism of PDA is reported to be dominated by hydrogen atom transfer from catechol groups.[15] A small amount of magnesium cations on clay surface may also act as an effective promoter for metal ion-coupled electron-transfer reactions,

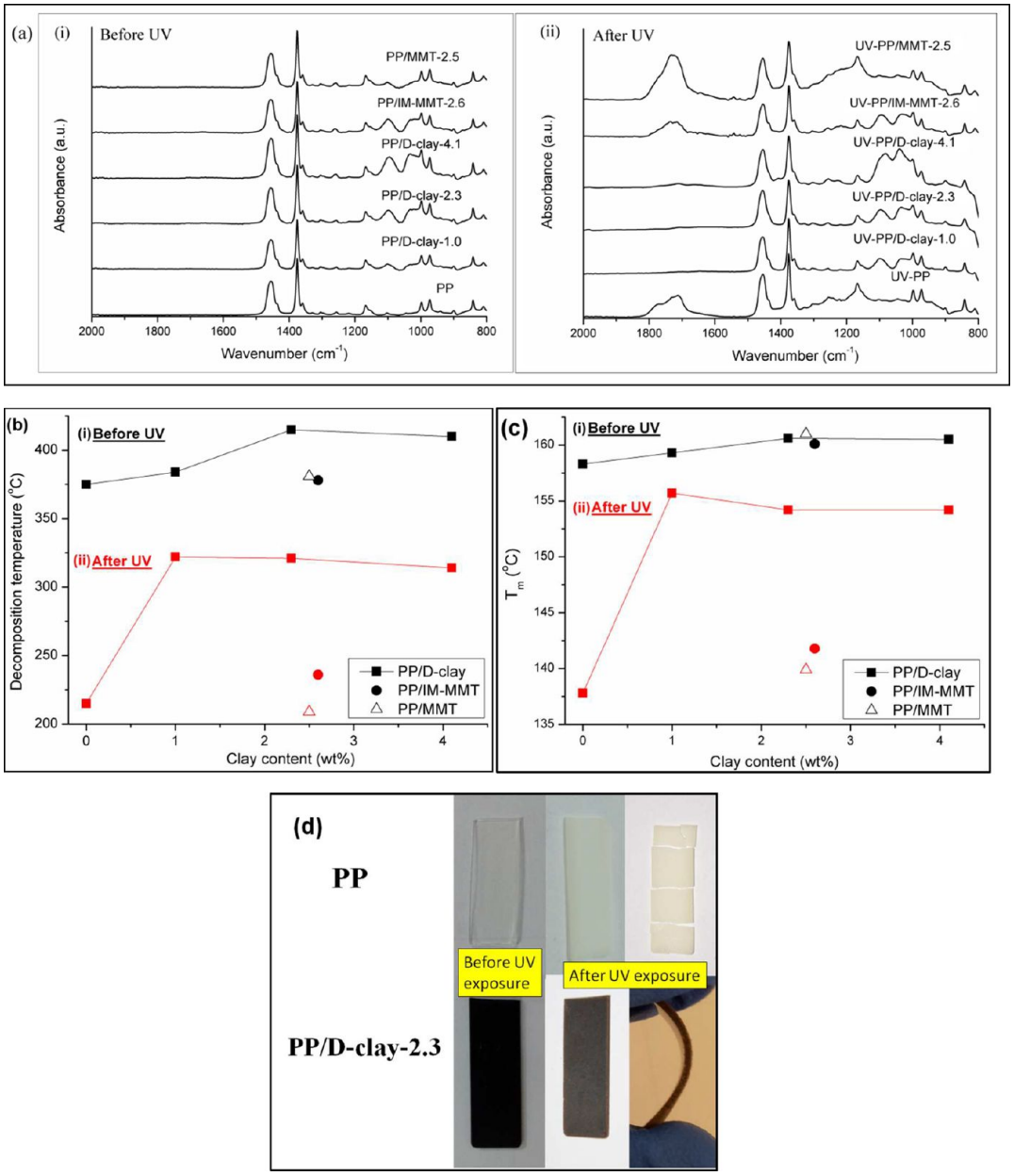

Figure 5. (a) FTIR spectra, (b) T_d in nitrogen, (c) T_m of PP, PP/D-clay, PP/IM-MMT, and PP/MMT before and after UV exposure for 3 weeks. The infrared spectra are normalized at 2722 cm^{-1} which is associated with CH_3 stretching and CH bending.[28] (d) Pictures showing films of PP and PP/D-clay-2.3 before and after 2 months of UV exposure.

accelerating the radical scavenging activity of PDA coating.[15] Therefore, the superior thermo-oxidative and UV stabilities of PP/D-clay nanocomposites can be attributed to abundant catecholamine moieties in PDA coating on the clay surface that act as efficient free-radical acceptors,[14,15] the relatively large surface area of the thin PDA coating that facilitates PDA to capture PP radicals, and probably also the presence of magnesium cations in the vicinity of PDA.

Tensile Properties of PP/D-Clay Nanocomposites. The motivation of this work was not merely to enhance free radical scavenging efficiency of PDA but to simultaneously reinforce and stabilize PP with a very low content of D-clay to achieve light-weight, strong yet durable thermoplastic materials. To demonstrate the reinforcement effect of D-clay, the tensile properties of PP and PP/clay nanocomposites are tabulated in Table 1. The typical tensile curves are given in Supporting Information (Figure S3). For all the nanocomposites, the stiffness and yield stress are enhanced by incorporating clay mineral, which is accompanied by a moderate reduction in elongation at break. The Young's modulus of PP/D-clay increases with increasing clay content, while the yield stress and elongation at break are independent of the clay content. Despite the slightly poorer clay dispersion state in PP/D-clay-2.3, its tensile properties are comparable with or slightly better than that of PP/IM-MMT at a similar clay loading. In comparison with neat PP, PP/D-clay-1.0 exhibits a 30 % increase in modulus accompanied by a 20 % increase in yield stress, although the crystallinity of PP/D-clay-1.0 is similar to that of neat PP (cf. Table S1, Supporting Information). The results imply that the interactions between the amine groups of $PPNH_2$ and D-clay as well as that between PP tails of $PPNH_2$ and the PP matrix may be fairly strong, giving rise to significant

dx.doi.org/10.1021/am3024405 | ACS Appl. Mater. Interfaces 2013, 5, 1302−1309

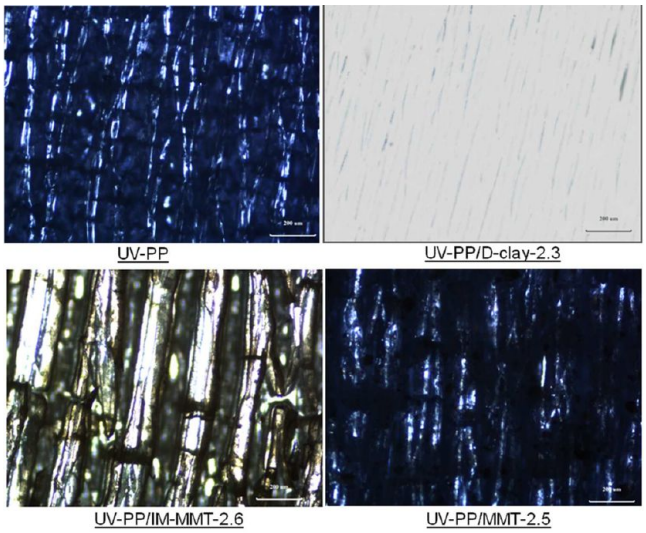

Figure 6. Optical micrographs showing specimen surface cracks (dark) after 2 months of UV exposure.

reinforcement effect at very low clay loadings. The PP oligomer used in this study has a fairly high molecular weight (M_n = 8000), which might allow the short PP chains attached on the clay entangle with long PP chains in the matrix or they might even co-crystallize, enhancing interfacial stress transfer. As the focus of this work is to demonstrate the simultaneous reinforcing and stabilizing effect of D-clay and reveal the mechanism for the impressive stabilizing effect of D-clay, the structure of the interface would be a subject for future study.

CONCLUSIONS

In summary, PP/D-clay nanocomposites were readily prepared with $PPNH_2$ as the compatibilizer. With the addition of a very small amount of D-clay, impressive enhancement of both thermal-oxidative stability and UV resistance of PP was observed owing to the radical scavenging capability of the PDA coating on clay. The strong radical scavenging capability of D-clay was further verified by the DPPH test. The results show that the radical scavenging efficiency of D-clay is much higher than that of PDA particles due to the larger surface area of the PDA coating on clay. The great improvement in photostability of PP/D-clay can also be attributed to the screening effect of melanin-like PDA coating, which is able to absorb the harmful irradiation and dissipates the energy via harmless paths. Other than the enhanced stabilities, tensile properties of PP/D-clay nanocomposites are also superior to that of neat PP; they are also better than that of the corresponding PP/organoclay nanocomposite probably due to the effective interfacial stress transfer between D-clay and PP matrix. The simultaneous enhancements in stiffness and stabilities make D-clay a promising nanofiller for polymers used in outdoor environments, where thermo-oxidative and UV stabilities play an important role for long-term applications.

Table 1. Tensile Properties of the PP and PP/Clay Nanocomposites

	Young's modulus (MPa)	yield stress (MPa)	tensile strength (MPa)	elongation at break (%)
PP	1730 ± 68	36.5 ± 0.7	47.9 ± 0.6	812 ± 31
PP/D-clay-1.0	2253 ± 142	43.9 ± 1.1	48.5 ± 0.5	573 ± 24
PP/D-clay-2.3	2342 ± 135	43.7 ± 0.7	46.1 ± 0.5	561 ± 48
PP/D-clay-4.1	2536 ± 148	43.2 ± 0.5	43.4 ± 0.3	524 ± 56
PP/IM-MMT-2.6	2309 ± 158	40.1 ± 0.8	40.1 ± 0.8	466 ± 116
PP/MMT-2.5	1936 ± 117	39.3 ± 0.9	44.2 ± 1.9	655 ± 98

ASSOCIATED CONTENT

Supporting Information

TEM images of $PPNH_2$/D-clay with different magnifications. DSC onset oxidation temperature (OOT) curves of PP and its nanocomposites. Typical tensile stress-strain curves of PP and its nanocomposites. Crystallinity of molded samples of PP and its nanocomposites. This material is available free of charge via the Internet at http://pubs.acs.org.

AUTHOR INFORMATION

Corresponding Author

*E-mail: asxhlu@ntu.edu.sg.

Notes

The authors declare no competing financial interest.

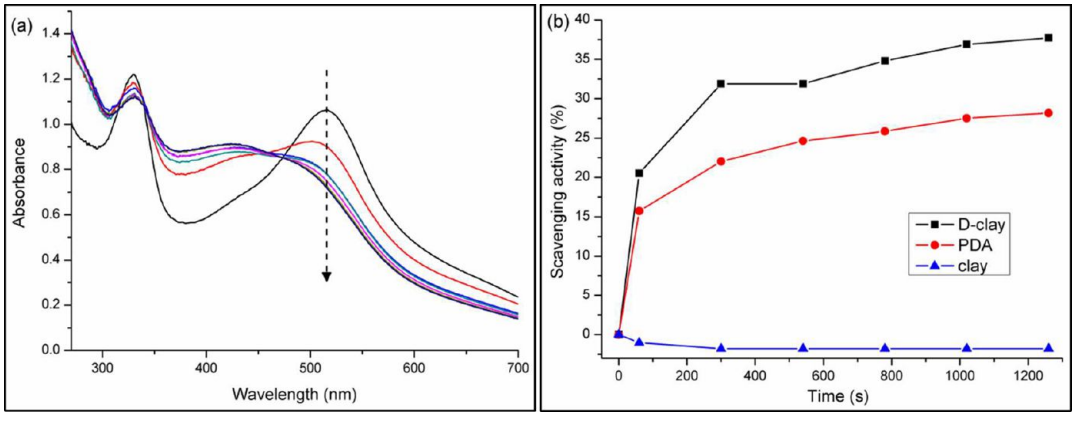

Figure 7. (a) UV-vis spectral change observed upon addition of D-clay to DPPH solution at 298 K. (b) DPPH radical scavenging activity of D-clay, PDA, and clay at different times.

■ ACKNOWLEDGMENTS

This work was supported by Science and Engineering Research Council of the Agency for Science, Technology and Research (A*Star) Singapore under Grant 092 137 0014. The electron microscopy and XRD work were performed at the Facility for Analysis, Characterization, Testing and Simulation (FACTS) in Nanyang Technological University, Singapore.

■ REFERENCES

(1) Pavlidou, S.; Papaspyrides, C. D. *Prog. Polym. Sci.* **2008**, *33*, 1119−1198.
(2) Chua, Y. C.; Lu, X. *Langmuir* **2007**, *23*, 1701−1710.
(3) Fogelström, L.; Malmström, E.; Johansson, M.; Hult, A. *ACS Appl. Mater. Interfaces* **2010**, *2*, 1679−1684.
(4) Podsiadlo, P.; Kaushik, A. K.; Arruda, E. M.; Waas, A. M.; Shim, B. S.; Xu, J.; Nandivada, H.; Pumplin, B. G.; Lahann, J.; Ramamoorthy, A.; Kotov, N. A. *Science* **2007**, *318*, 80−83.
(5) Dharaiya, D.; Jana, S. C. *Polymer* **2005**, *46*, 10139−10147.
(6) Morlat, S.; Mailhot, B.; Gonzalez, D.; Gardette, J. L. *Chem. Mater.* **2004**, *16*, 377−383.
(7) Dominkovics, Z.; Hári, J.; Fekete, E.; Pukánszky, B. *Polym. Degrad. Stab.* **2011**, *96*, 581−587.
(8) Yang, L.; Phua, S. L.; Teo, J. K. H.; Toh, C. L.; Lau, S. K.; Ma, J.; Lu, X. *ACS Appl. Mater. Interfaces* **2011**, *3*, 3026−3032.
(9) Dreyer, D. R.; Miller, D. J.; Freeman, B. D.; Paul, D. R.; Bielawski, C. W. *Langmuir* **2012**, *28*, 6428−6435.
(10) Lee, H.; Dellatore, S. M.; Miller, W. M.; Messersmith, P. B. *Science* **2007**, *318*, 426−430.
(11) Waite, J. H. *Nat. Mater.* **2008**, *7*, 8−9.
(12) Meredith, P.; Sarna, T. *Pigm. Cell Res.* **2006**, *19*, 572−594.
(13) Shanmuganathan, K.; Cho, J. H.; Iyer, P.; Baranowitz, S.; Ellison, C. J. *Macromolecules* **2011**, *44*, 9499−9507.
(14) Ju, K. Y.; Lee, Y.; Lee, S.; Park, S. B.; Lee, J. K. *Biomacromolecules* **2011**, *12*, 625−632.
(15) Kawashima, T.; Ohkubo, K.; Fukuzumi, S. *J. Phys. Chem. B* **2010**, *114*, 675−680.
(16) Riesz, J.; Sarna, T.; Meredith, P. *J. Phys. Chem. B* **2006**, *110*, 13985−13990.
(17) Lawrie, K. J.; Meredith, P.; McGeary, R. P. *Photochem. Photobiol.* **2008**, *84*, 632−638.
(18) Yah, W. O.; Xu, H.; Soejima, H.; Ma, W.; Lvov, Y.; Takahara, A. *J. Am. Chem. Soc.* **2012**, *134*, 12134−12137.
(19) Jaber, M.; Bouchoucha, M.; Delmotte, L.; Méthivier, C.; Lambert, J. F. *J. Phys. Chem. C* **2011**, *115*, 19216−19225.
(20) Jaber, M.; Lambert, J. F. *J. Phys. Chem. Lett.* **2010**, *1*, 85−88.
(21) Lee, H.; Scherer, N. F.; Messersmith, P. B. *Proc. Natl. Acad. Sci. U. S. A.* **2006**, *103*, 12999−13003.
(22) Podsiadlo, P.; Liu, Z.; Paterson, D.; Messersmith, P. B.; Kotov, N. A. *Adv. Mater.* **2007**, *19*, 949−955.
(23) Yang, L.; Yee, W. A.; Phua, S. L.; Kong, J.; Ding, H.; Cheah, J. W.; Lu, X. *RSC Adv.* **2012**, *2*, 2208−2210.
(24) Yang, L.; Kong, J.; Yee, W. A.; Liu, W.; Phua, S. L.; Toh, C. L.; Huang, S.; Lu, X. *Nanoscale* **2012**, *4*, 4968−4971.
(25) Phua, S. L.; Yang, L.; Toh, C. L.; Huang, S.; Tsakadze, Z.; Lau, S. K.; Mai, Y.-W.; Lu, X. *ACS Appl. Mater. Interfaces* **2012**, *4*, 4571−4578.
(26) Zhao, H.; Li, R. K. Y. *Polymer* **2006**, *47*, 3207−3217.
(27) Chua, Y. C.; Wu, S.; Lu, X. *J. Nanosci. Nanotechnol.* **2006**, *6*, 3985−3988.
(28) Bezati, F.; Massardier, V.; Balcaen, J.; Froelich, D. *Polym. Degrad. Stab.* **2011**, *96*, 51−59.
(29) Xu, L.; Nakajima, H.; Manias, E.; Krishnamoorti, R. *Macromolecules* **2009**, *42*, 3795−3803.
(30) Ku, K. H.; Kim, S. C. *J. Appl. Polym. Sci.* **2009**, *113*, 1539−1549.
(31) Százdi, L.; Pukánszky, B., Jr.; Földes, E.; Pukánszky, B. *Polymer* **2005**, *46*, 8001−8010.
(32) Socrates, G., *Infrared and Raman characteristic group frequencies : tables and charts*, 3rd ed.; Wiley: New York, 2001.
(33) Mittal, V. *Eur. Polym. J.* **2007**, *43*, 3727−3736.
(34) Guadagno, L.; Naddeo, C.; Raimondo, M.; Gorrasi, G.; Vittoria, V. *Polym. Degrad. Stab.* **2010**, *95*, 1614−1626.
(35) Kumar, A. P.; Depan, D.; Singh Tomer, N.; Singh, R. P. *Prog. Polym. Sci.* **2009**, *34*, 479−515.